Computer simulated alternative modes of U wave genesis

(short title: Alternative modes of U wave genesis)

Matjaž Depolli [1], Viktor Avbelj, Roman Trobec

Department of communication systems, Jozef Stefan Institute
Jamova 39, 1000 Ljubljana, Slovenia

Authors

Matjaž Depolli, Ph.D. student
junior researcher

Viktor Avbelj, Ph.D.
senior researcher

assis. prof. Roman Trobec, Ph.D.
senior researcher

Acknowledgment

The authors acknowledge financial support from the Slovenian Research Agency under grant P1-0095.

[1] Corresponding author: Tel.: +386 1 4773135; fax: +386 1 4773111.
E-mail address: matjaz.depolli@ijs.si

Abstract

Objective: Several hypotheses for the origin of the U wave in electrocardiograms have been proposed. We have set to explore and test alternative modes for U wave genesis via a computer simulations.

Methods and Results: A spatial model of a left ventricle has been constructed from twelve layers, composed of cubic cells. Each cell is assigned its own time dependent action potential with its own contribution to the electrical potential at arbitrary points where ECGs are measured. Simulated ECGs show that U waves can be generated using various combinations of action potentials across the different layers of the ventricular wall. We demonstrate a new mode of U wave genesis, even with small differences in the repolarization.

Conclusion: The U wave can be generated in the presence of strong intercellular coupling. Myocardial layers with prolongated action potentials, like M cells, are not necessarily needed for U wave genesis.

Keywords

U wave, ECG, action potential, repolarization, myocardium, computer simulation

1 Introduction

The origin of the U wave in the electrocardiogram, first described by Willem Einthoven at the beginning of the 20^{th} century, is still debated. Several hypotheses have been proposed [1], three of which are most frequently quoted. The first hypothesis attributes U wave genesis to the late repolarization of Purkinje fibers [2], the second to mechanoelectrical feedback [3,4], and the last to the late repolarization of cells in mid-myocardium (M cells) [5,6].

Recently a novel view of the M cell hypothesis was presented, proposing that T and U waves form a continuum and can both be expected to occur in every ECG [7,8]. The end of the T wave is taken as the residual of cancellation of opposing potential contributions throughout the myocardium during the repolarization. The U wave arises when some imbalance of potentials appears in the late repolarization because of the prolongated repolarization of M cells.

It is known that myocardial cell preparations from different depths of the ventricular wall show substantial differences in action potential duration (APD) [6,9], which creates a transmural gradient in the repolarization. The measurements in the intact human heart show much smaller differences [10], however, the *in vivo* measurements should be interpreted with great caution [11]. There are also theoretical indices, that transmural differences should be smaller than measured *in vitro* [9,12], due to the absence of cell coupling and electrotonic current flow in these measurements.

Considering the properties of the intact heart we supposed that there should be solutions for U wave genesis other than that proposed in [7], which uses the M cells hypothesis, or that proposed in [13], which uses additional after-potentials. In this paper we present an alternative mode of U wave genesis through a simulation experiment. We show that U waves can be generated even if the transmural gradient in the repolarization is almost absent and exhibits no maximum originating in M cells.

In the next section the simulation experiment is described. In Results, previously simulated results are verified and alternative modes of U wave genesis are shown. In the Discussion, the mechanism of U wave genesis and possible limitations of the presented work are analyzed. The paper concludes with an overview of the results and further work.

2 Methods

2.1 Heart model

We constructed a heart model using a three-dimensional grid of cubic cells with a volume of 1 mm^3, shown in Figure 1. Cells are arranged in a stylized shape of the left ventricle, with all other parts of the heart omitted. Although arbitrary shapes can be created, we constrained ourselves to shapes used in [7], in order to be able to reproduce their experiments. Three models of different complexity are used. The simplest is a string of 12 cells, representing a column

of transmural tissues of the left ventricular wall. Each cell represents a different myocardial layer, from the inner endocardium, through ten layers of mid-myocardium, to the surface epicardium.

The slice model is an extension of the string model, stylized as an oval, with the semimajor and semiminor axes of the outermost layer 35 and 30 millimeters, respectively. Only 5/8 of the oval are considered, which results in 1194 cells. The oval slice lies in the plane defined by the standard ECG leads (V1 – V6). The spatial model is obtained by rotating the slice model around its major axis to create a cup-like, three-dimensional ventricle, comprising 65628 cells.

The layered myocardium enables different action potentials (APs) to be assigned to each of twelve layers. APs are modeled as a product of two sigmoid functions and an exponential function, as proposed in [14]:

$$\begin{aligned} A(t) &= \tfrac{1}{1+e^{-k_1 t}} \\ B(t) &= k_2((1-k_3)e^{-k_4 t} + k_3)e^{-k_5 t} \\ C(t) &= \tfrac{1}{1+e^{k_6(t-k_7)}} \\ AP(t) &= A(t) \times B(t) \times C(t) \ , \end{aligned} \tag{1}$$

where component $A(t)$ controls the initial upstroke (phase 0), $B(t)$ the immediate fast repolarization and the AP plateau (phases 1 and 2, respectively), and $C(t)$ the repolarization part (phase 3). Because of the characteristics of

exponential functions, however, the whole AP curve is influenced to some extent by all the components. Examples of AP curves for layers 1 and 12 with their phases are shown in the upper left corner of Figure 1. Activation time (AT) represents delay between the myocardium excitation start and individual cell activation. Repolarization time (RT) is a sum of AT and APD and is the measure of total delay between the myocardium excitation start and individual cell repolarization end.

The layered model enables the simulation of faster conduction through the Purkinje fibers with implementing faster longitudinal conduction between cells of the same layer (along the wall) than transversal conduction between cells of different layers (across the wall). A limited control of intercellular coupling is also possible within the layered model. Cells of the same layer are implicitly strongly coupled because they share the same AP shape. Intercellular coupling between cells of different layers is controlled by differences in corresponding APs.

2.2 Excitation model

The excitation sequence defines the delay in excitation for each cell relative to the excitation start. Excitation is triggered in the endocardium cell in case of the string model and in eight neighboring endocardium cells in the case of the slice and spatial model. The arrow in Figure 1 denotes the excitation area. An example of the excitation sequence is shown in the same figure on the cut

myocardial wall with levels of gray.

Excited cells behave as sources of electrical potential determined by their AP functions. Every excited cell stimulates its neighboring non-excited cells to become excited with a small delay, which depends on the layer of the neighboring cell and its position relative to the excited cell. If cells are from different layers, the delay is 2 ms, which translates into transversal conduction velocity of 0.5 m/s. If cells belong to the same layer, the delay is 1/3 ms, which translates into longitudinal conduction velocity of 3 m/s. Both velocities are in accordance with measured values on myocardial tissue [15][16, p. 111–116]. The delay, multiplied by the distance between the observed cells, yields different AT for each cell. Since a cubic grid is used for cells, the immediate neighbors of cells, those with coincident faces, are located at a distance of 1 mm, neighbors with coincident edges at $\sqrt{2}$ mm, and neighbors with coincident corners at $\sqrt{3}$ mm.

2.3 ECG model

The ECG is a view on the electrical heart activity from the outside. Electric potentials are generated on observation points located at standard places (V1 – V6). In the case of the slice and spatial models, six observation points are selected around the model, 4 cm away from the epicardial layer, at angles $-120°$ (V1) to $30°$ (V6), in steps of $30°$, mimicking the real ECG leads placing (see Figure 1). In the case of the string model, only lead V2 is used, because it

lies on the string model axis. The string model, however, features additional lead, V_∞, which lies on the same axis but far away from the epicardial layer (1000 m was used in our simulation), so that distances between layers are negligible in comparison to the distance of this lead. V_∞ records behavior in which only the difference between the endocardial and epicardial layers produce observable effects, because contributions of M cells are canceled, as shown in [7].

We assume formation of a dipole between cell i and its immediate neighborhood Ω, in the same way as in [17], which includes only neighbors with coincident faces, i.e., 2, 4, and 8 neighbors for the string, slice, and spatial models. Electrical potential differences between cells arise from the differences between cell APs. Dipole moment $\mathbf{D}_i$ is proportional to the vector sum of differences in potentials V:

$$\mathbf{D}_i(t) \propto \sum_{j \in \Omega(i)} \left(V_i(t) - V_j(t)\right) . \tag{2}$$

ECG leads are simulated as observation points at which the dipole potential is measured. We use a directional vector $\mathbf{R}_{i,P}$ from the cell of dipole origin i to the observation point P to calculate the magnitude of the dipole contribution to the potential $V_{i,P}$ recorded in P. $V_{i,P}$ is proportional to the cosine of the angle ϕ between $\mathbf{D}_i$ and $\mathbf{R}_{i,P}$ and inversely proportional to the square of the distance between the cell of origin and the observation point. The total potential V_P is the sum of contributions of all N cells. Adding the time variability of the

dipole moment we obtain:

$$V_P(t) \propto \sum_{i=1}^{N} \frac{|\mathbf{D}_i(t)| \cdot \cos\phi}{|\mathbf{R}_{i,P}|^2} \ , \tag{3}$$

which gives the simulated ECG of the lead placed at observation point P.

3 Results

3.1 Model verification

We compared our simulation results to results presented in [7]. Equation 1 was used to model endocardial, epicardial, and the longest 5^{th} M cell layer. Coefficients were found by a search with a differential evolution [18] that evolved AP shapes. The rest of the M cell APs were scaled in time by a factor k_t: $AP_i(t) = AP_5(t \cdot k_t)$, from 5^{th} M cell AP, to reach the desired durations. Resulting coefficients are given in Table 1. First four coefficients are not included since their values are the same for all APs: $k_1 = 2.5$, $k_2 = 100$, $k_3 = 0.9$, $k_4 = 0.1$. The table also includes APD at 90% repolarization (APD_{90}) and repolarization time at 90% repolarization(RT_{90}). Note that APs converge towards the resting potential, therefore, we take 90% repolarization as finished.

APs, generated using coefficients from Table 1, are shown in Figure 2(a), along with the ECG, simulated on the string model. The simulated ECG accords well with the simulated ECG presented in [7].

3.2 A new approach to U wave genesis

After model verification, we considered our model elaborate enough to be able to explore other possible modes of U wave genesis. Differential evolution was used again, to tackle the inverse problem of searching for the possible inputs to the simulator, that produce an ECG with a visible U wave. A search on a limited search space, allowing only sets of APs to change, and keeping the geometry of the model, conduction velocities, and positions of ECG leads as described before, resulted in the U wave being reproduced in many different ways. Three examples are given in Figure 2. The already described upper set of APs, used for verification, was generated with coefficients from Table 1. In the middle set, all ten M cell layers (mid) are assigned identical APs. In the lower set, mid layer APs are linearly interpolated between the endocardial layer (endo) with APD_{90} = 340 ms, 5^{th} layer (mid) with APD_{90} = 405 ms, and epicardial layer (epi) with APD_{90} = 340 ms. M cell layers in the upper and lower set thus form a maximum in the 5^{th} layer.

Such a myriad of solutions motivated us to pursue U wave genesis in the absence of a maximum in M cell repolarization time, which was implemented with the selection of coefficients of Equation 1 in such a way that all M cell APs are evenly distributed between the endocardial and epicardial APs. Coefficients k_1, k_2, k_3, and k_4 are the same as defined in previous section, the remainder are given in Table 2. Such a construction of APs does not allow any

significant differences in potentials of neighboring layers, as is expected to be the effect of strong intercellular coupling.

It can be seen from Figure 3(a) that action potential durations (APD_{90}) of the neighboring myocardial layers are similar, with the longest in endocardium and the shortest in epicardium. On introducing AT we obtain a situation, in which dispersion of repolarization time (RT_{90}) is very small (see Figure 3(b)). Simulated ECG on the string model is shown on the lower part of the same figure. The repolarization of epicardium precedes that of endocardium by 2 ms. The orientation of the gradient is the same as that reported for human heart measurements *in vivo* [20], and is opposite to that from the simulation presented in [7]. ECGs, simulated on the slice and spatial models, are shown separately on Figure 4 with a measured ECG, analyzed previously in [19], for a reference. Morphology of the simulated ECGs differ from the measured ECGs mostly in T wave due to the use of simplified AP model.

4 Discussion

4.1 Heart model

For better understanding of the simulation, the model of the ventricular wall can be thought of as a set of string models stacked on an elliptical path, while the spatial model can be thought of as a set of rotated slice models. If the excitation started in all the endocardial cells at once, all string responses would

be synchronized in time. Simulated ECGs would record the sum of all string responses, and therefore differ only in amplitudes. String responses, however, are delayed by their corresponding AT. Excitation does not start in the whole endocardium at once but is delayed along the wall, reaching a maximum delay of 25.5 ms in the part of the wall opposite to the excitation starting point. Observing such a model from different angles results in a more complicated cancellation scheme, that can shift T and U waves in time, and change their shapes.

All the models presented exhibit uniform wall thickness and missing parts of a heart with their conduction paths, e.g. right ventricle. Some preliminary experiments show that the influence of the model shape on the simulated ECG is minimal, however, further work is needed in this area.

Our simulations assume a homogeneous APs for the whole set of cells belonging to the same layer (e.g. epicardial cells in base and apex exhibit the same AP morphology). Together with the cells' excitation sequence, this translates into fixed RT gradient along the wall, with RT linearly dependent on the distance from the excitation area node. This prevents the investigation of another possible mode for U wave genesis – the repolarization gradient between the base and the apex [9].

We use a simple heart model inside an infinite homogeneous volume conductor, which enables a fast search through AP combinations that result in the

correctly shaped ECGs. If more elaborate models were used (inhomogeneous, anisotropic volume conduction in heart and torso model), we expect that the results would be similar [16, p. 221–230].

4.2 AP model

The AP model defined by Equation 1 was used in our work because of its simplicity, having only three parameters to control phases 2 and 3. Although it proved powerful enough to model different scenarios of U wave genesis, some drawbacks emerged. Two most prominent one is the inability of the model to independently control AP phases 2 and 3. Such ability would allow reshaping of APs that would independently change the form and position of T and U waves. For example, smaller differences between the APs in phase 2 than those shown in Figure 3(b) would result in shorter T wave. It can be expected that such extension of the AP model would generate further possibilities for U wave genesis.

We also tried to model the measured APs published in [6], using the same searching procedure as in model verification from the previous section. Model Equation 1 has not produced useful results because it was unable to generate APs that would fit the measured APs with required accuracy. A more complex AP model is needed for testing whether APs, shaped similar to those published in [6], could generate the U wave directly.

4.3 U wave genesis

To show the main feature of the proposed U wave genesis consider the string model with leads V2 and V_∞, that both lie on the string model axis. ECGs, simulated separately on each lead, with coefficients from Table 2 are almost identical, with correlation coefficient 0.99992. This differs from the findings in [7], where a U wave was generated only on the lead near the model wall. This was a consequence of the prolongated APs of M cells, which have an effect only observable at very short distances, consequently, the U wave disappears at longer distances.

U wave genesis, proposed in this paper, bases on the difference between endocardial and epicardial APs, since it is observable at distances that are several orders of magnitude greater than the thickness of myocardium wall. A graphical explanation of how positive T and U waves can be formed by a difference between two APs, obtained according to Equation 1, is shown in Figure 5. The minimum difference occurs where APs converge, or touch each other. AP curves can even intersect twice, creating a negative minimum.

5 Conclusion

We have created a three-dimensional model of a left ventricle for a computer simulation of ECGs, including U wave genesis, by a variety of different AP sets. We reproduced results from [7] and confirmed that U wave genesis may

be due to prolongated APs of M cells.

Additionally, we generated U waves with almost no transmural gradient in the repolarization and with no maximum in mid-myocardium repolarization time, thus making simulations in accordance with the *in vivo* heart measurements [10]. We were able to do so in spite of the simple and rigid AP model, that should be improved for further investigation.

It is worth noting that our findings do not exclude any of the other U wave hypotheses mentioned before, they merely provide another one. We conclude that the transmural gradient in the repolarization is sufficient for U wave genesis but not necessarily its sole cause. Also, we can only speculate on the reasons behind the repolarization gradient. The gradient may be due to intrinsic differences in APs between the endocardium and epicardium, or due to differences arising from mechanoelectrical feedback. One can even assume that APs adapt in time to the current status of the heart in order to optimize its work. The further investigation is needed to elucidate the mentioned hypotheses.

6 Acknowledgment

The authors acknowledge financial support from the Slovenian Research Agency under grant P1-0095.

References

[1] Surawicz B: U wave: Facts, hypotheses, misconceptions, and misnomers. J Cardiovasc Electrophysiol 1998; 9:1117–1128.

[2] Watanabe Y: Purkinje repolarization as a possible cause of the U wave in the electrocardiogram. Circulation 1975; 51:1030–1037.

[3] Lab MJ: Contraction-excitation feedback in myocardium. Physiological basis and clinical relevance. Circ Res 1982; 50:757–766.

[4] Franz MR: Mechano-electrical feedback in ventricular myocardium. Cardiovasc Res 1996; 32:15–24.

[5] Antzelevitch C, Sicouri S: Clinical relevance of cardiac arrhythmias generated by afterdepolarizations. Role of M cells in the generation of U waves, triggered activity and torsade de pointes. J Am Coll Cardiol 1994; 23:259–277.

[6] Druin E, Charpentier F, Gauthier C, Laurent K, Le Marec H: Electrophysiologic characteristics of cells spanning the left ventricular wall of human heart: Evidence for presence of M cells. J Am Coll Cardiol 1995; 26:185–192.

[7] Ritsema van Eck HJ, Kors JA, van Herpen G: The U wave in the electrocardiogram: A solution for a 100-year-old riddle. Cardiovasc Res 2005; 67:256–262.

[8] Ritsema van Eck HJ, Kors JA, van Herpen G: Dispersion of repolarization, myocardial iso-source maps, and the electrocardiographic T and U waves. J Electrocardiol 2006; 39:96–100.

[9] Taggart P, Sutton P, Opthof T, Coronel R, Kallis P: Electrotonic cancellation of transmural electrical gradients in the left ventricle in man. Prog Biophys Mol Biol 2003; 82:243–254.

[10] Taggart P, Sutton PM, Opthof T, Coronel R, Trimlett R, Pugsley W, Kallis P: Transmural repolarisation in the left ventricle in humans during normoxia and ischaemia. Cardiovasc Res 2001; 50:454–462.

[11] Antzelevitch C: Transmural dispersion of repolarization and the t wave. Cardiovasc Res 2001; 50:426–431.

[12] Conrath CE, Opthof T: The patient U wave. Cardiovasc Res 2005; 67:184–186.

[13] di Bernardo D, Murray A: Origin on the electrocardiogram of U-waves and abnormal U-wave inversion. Cardiovasc Res 2002; 53:202–208.

[14] Wohlfart B: A simple model for demonstration of SST-changes in ECG. Eur Heart J 1987; 8:409–416.

[15] Taggart P, Sutton PM, Opthof T, Coronel R, Trimlett R, Pugsley W, P. Kallis: Inhomogeneous transmural conduction during early ischaemia in patients with coronary artery disease. J Mol Cell Cardiol 2000; 32:621–630.

[16] Macfarlane PW, Lawrie TDV, eds. Comprehensive Electrocardiology: Theory and Practice in Health and Disease. 1st Edition. Vol. 1. Pergamon Press, New York; 1989.

[17] Miller WT, Geselowitz DB: Simulation studies of the electrocardiogram. I. The normal heart. Circ Res 1978; 43:301–315.

[18] Storn R, Price K: Differential evolution - a simple and efficient adaptive scheme for global optimization over continuous spaces. Tech. Rep. TR-95-012Berkeley, CA (1995).

[19] Avbelj V, Trobec R, Gersak B: Beat-to-beat repolarisation variability in body surface electrocardiograms. Med Biol Eng Comput 2003; 41:556–560.

[20] Franz MR, Bargheer K, Rafflenbeul W, Haverich A, Lichtlen PR: Monophasic action potential mapping in human subjects with normal electrocardiograms: direct evidence for the genesis of the T wave. Circulation 1987; 75:379–386.

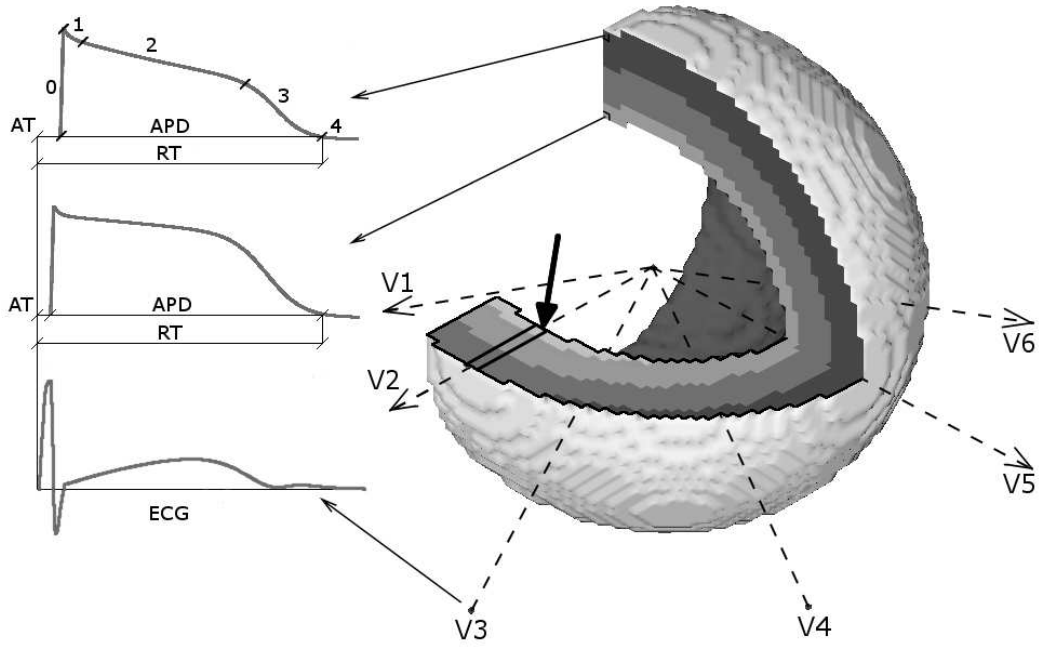

Figure 1. Spatial model of the left ventricle. The string model is the transmural column and the slice model is the central slice, both outlined in bold. ECG leads are in the plane of the slice model, with the string model on the virtual line connecting V2 with the model center. The thick arrow points to the excitation trigger area; the excitation sequence is shown on the cut myocardial wall with levels of gray. On the left, APs for epicardium (top) and endocardium (middle) with corresponding phases, AT, APD, and RT are shown, together with simulated ECG on V3 (bottom).

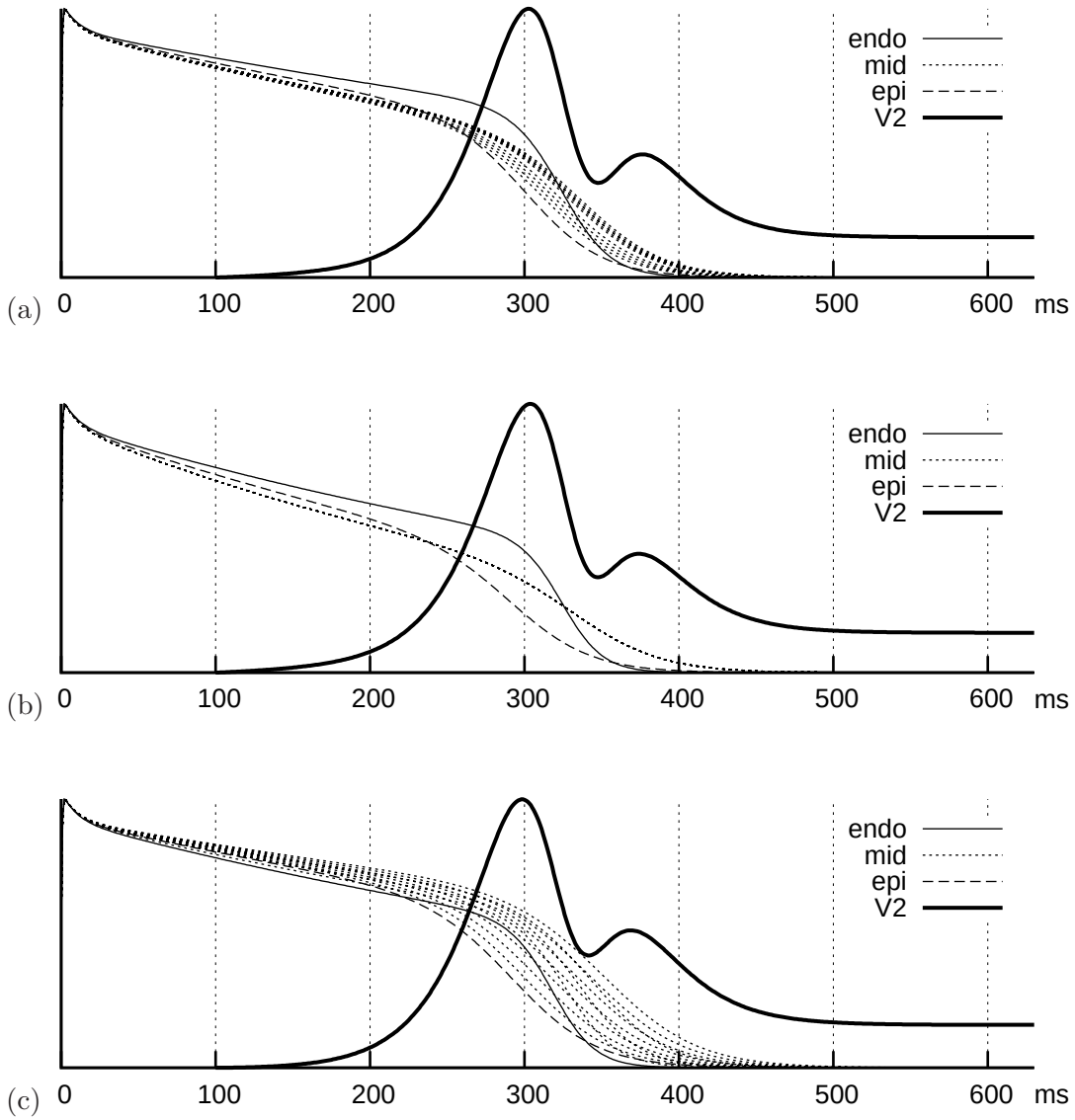

Figure 2. Three different sets of APs that generate similarly shaped T and U waves on the slice model, with the simulated ECG on lead V2: (a) APs that correspond to Table 1; (b) identical APs for M cell layers; (c) linearly interpolated APs with maximal $APD_{90} = 405$ ms at the 5^{th} layer. Scale of amplitude for APs is arbitrary but the same for all figures. Simulated ECGs are scaled and offset in amplitude, and drawn from 100 ms onwards, to fit in figures.

Table 1
Coefficients of Equation 1 used to reproduce results from [7].

layer	k_5	k_6	k_7	k_t	APD_{90}	RT_{90}
1	0.00124	0.0635	325.5	-	350.8	350.8
2	0.00162	0.0367	340.7	0.963	372.6	374.6
3	0.00162	0.0367	340.7	0.989	374.6	378.6
4	0.00162	0.0367	340.7	0.988	376.6	382.6
5	0.00162	0.0367	340.7	1.000	378.6	386.6
6	0.00162	0.0367	340.7	0.988	374.6	384.6
7	0.00162	0.0367	340.7	0.976	370.7	382.7
8	0.00162	0.0367	340.7	0.958	364.8	378.8
9	0.00162	0.0367	340.7	0.946	360.8	376.8
10	0.00162	0.0367	340.7	0.935	356.9	374.9
11	0.00162	0.0367	340.7	0.923	352.9	372.9
12	0.00148	0.0400	304.0	-	342.1	364.1

Table 2
Coefficients of Equation 1 used for U wave genesis without prolonged M cell APs.

layer	k_5	k_6	k_7	APD_{90}	RT_{90}
1	0.000500	0.0287	422.1	484.4	484.4
2	0.000587	0.0293	422.2	481.9	483.9
3	0.000673	0.0299	422.3	479.4	483.4
4	0.000760	0.0305	422.4	477.0	483.0
5	0.000847	0.0311	422.5	474.7	482.7
6	0.000933	0.0316	422.6	472.5	482.5
7	0.001020	0.0322	422.7	470.3	482.3
8	0.001106	0.0328	422.8	468.2	482.2
9	0.001193	0.0334	422.9	466.2	482.2
10	0.001280	0.0339	423.0	464.3	482.3
11	0.001366	0.0345	423.1	462.4	482.4
12	0.001453	0.0351	423.2	460.5	482.5

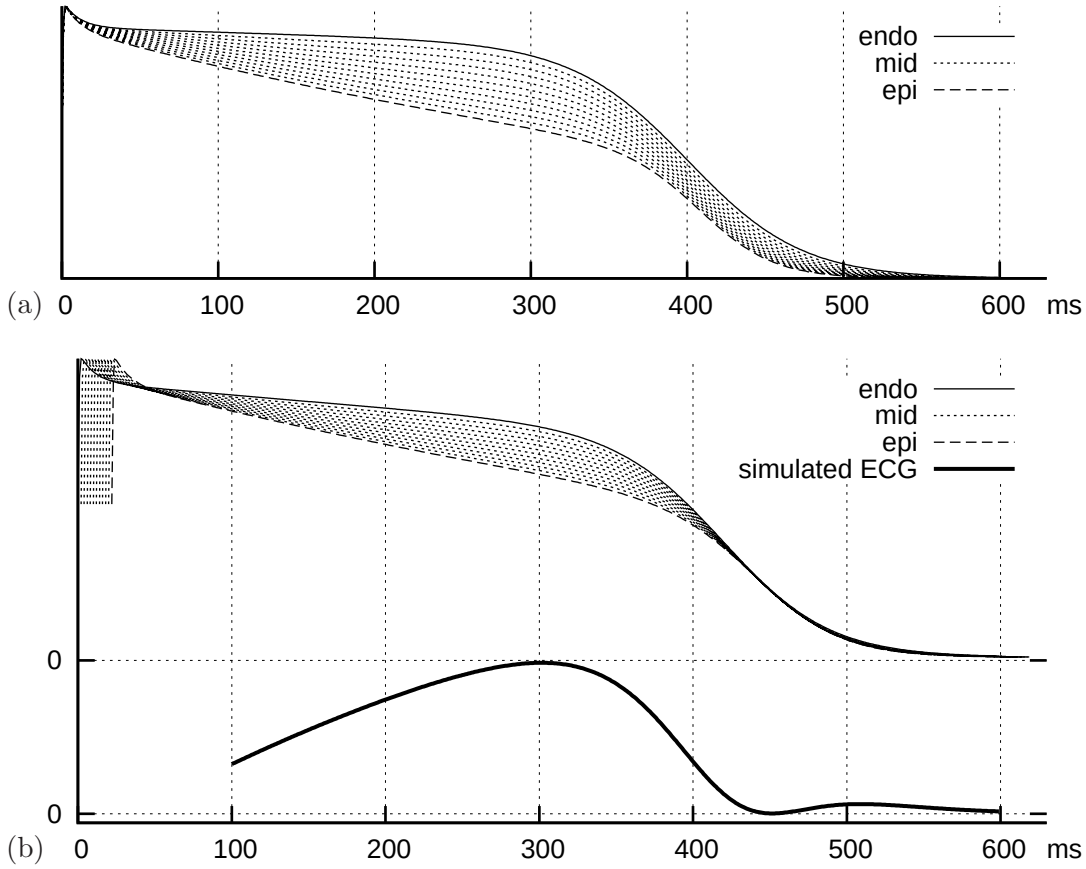

Figure 3. Twelve AP curves for a new mode of U wave genesis 3(a), the same AP curves shifted by corresponding activation time - in 2 ms steps 3(b) with the corresponding ECG, simulated on the string model.

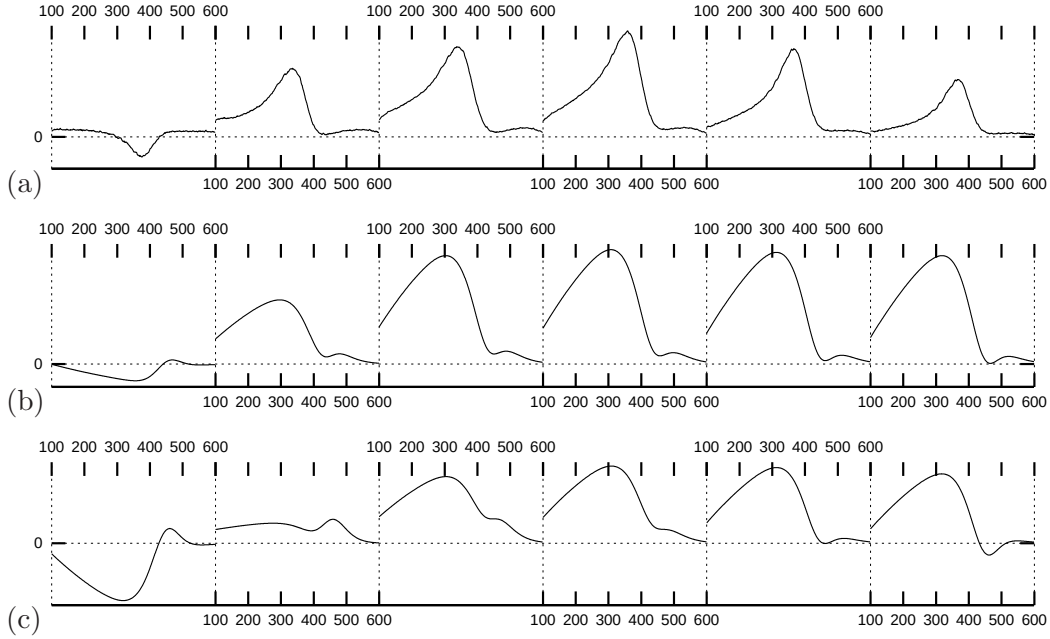

Figure 4. Measured V1 – V6 leads (a), and simulated ECG with the new mode of U wave genesis on the slice model (b) and on the spatial model (c).

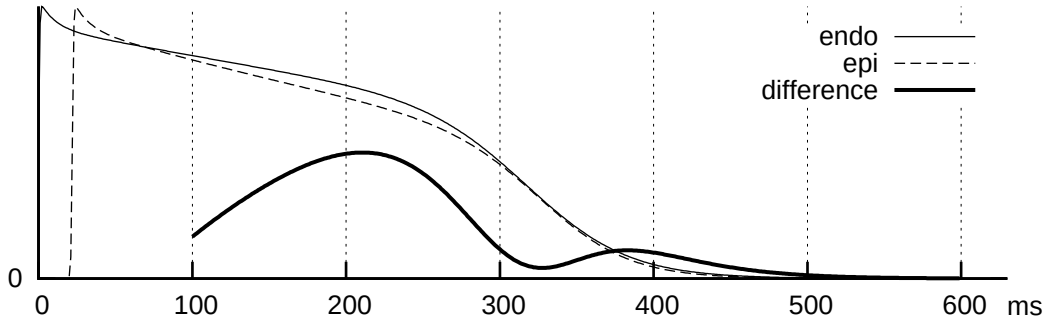

Figure 5. The U wave generated as a difference between two APs. The difference is magnified ten times.